Carbon Science

Vol. 1, No. 2 September 2000 pp. 53-59

Synthesis of High Purity Multiwalled and Singlewalled Carbon Nanotubes by Arc-discharge

Keun Soo Kim, Young Soo Park, Kay Hyeok An, Hee Jin Jeong, Won Seok Kim, Young Chul Choi, Seung Mi Lee, Jeong Mi Moon, Dong Chul Chung*, Dong Jae Bae, Seong Chu Lim, Young Seak Lee and Young Hee Lee♠**

Department of Semiconductor Science and Technology, Department of Physics, and Semiconductor Physics Research Center, Jeonbuk National University, Jeonju 561-756, Korea

*Division of Information, Communication, and Computer Engineering, Woosuk University, Wanju 561-701, Korea

**Department of Chemical Enginnering, College of Enginnering Sunchon National University, Sunchon 540-742, Korea

♠e-mail: *leeyh@sprc2.chonbuk.ac.kr*

(Received August 1, 2000; accepted September 5, 2000)

Abstract

The synthetic methods for high yield of multiwalled carbon nanotube (MWNT) and singlewalled carbon nanotube (SWNT) with high purity by arc discharge have been investigated. MWNTs were synthesized under different pressures of helium and the gas mixture of argon and hydrogen. Relatively high pressure of 300-400 torr was required for high yield MWNTs synthesis at low bias voltage of about 20 V and 55 A, whereas low pressure of about 100 torr was required for SWNTs. The introduction of hydrogen gases during the synthesis of MWNTs improved the yield and purity of the samples. The SWNTs were synthesized by the assistance of a small amount of mixture of transition metals, which played as a catalyst during the formation process. The purity and yield of SWNTs were higher at a lower pressure and enhanced by mixing more components of the transition metals.

Keywords : *Multiwalled carbon nanotubes, singlewalled carbon nanotubes, arc-discharge*

1. Introduction

Since carbon nanotubes (CNTs) were discovered by Iijima [1], they have been known to have superb applications such as the hydrogen storage [2-3], the electrode for supercapacitor and battery [4-6], AFM/STM tips [7-9], single electron transistor [10-12], and field emission display [13-16]. The CNTs have been synthesized by dc arc discharge[16-19], laser ablation [20,21], pyrolysis of hydrocarbon [22-24], and chemical vapor deposition (CVD) [13-15]. Among them, the arc discharge has been known very simple and cheap, and have a merit to make massive production. However the method reveals lower yield of CNTs in the products than other methods.

A lot of undisirable carbonaceous particles such as fullerenes, nanoparticles, and amorphous phases are always contained in the soot in addition to CNTs in arc discharge. Highly purified CNTs are generally required for further sophisticated measurements and practical applications. The various purification techniques, such as filtration, chromatography, centrifugation, gas phase oxidation, and chemical purification, have been tried to purify the CNTs [25-28]. Although the CNTs are separated to some extent from carbonaceous particles, the yield is very low in most cases. These purification processes act as a large barrier to several applications of the CNTs.

In this study, we have investigated the optimum synthetic conditions of arc-discharge in order to obtain directly high purity and high yield of multiwalled carbon nanotubes (MWNTs) and singlewalled carbon nanotubes (SWNTs). In synthesizing CNTs by arc discharge, the shape and composition of the products depend strongly on the experimental conditions. Therefore, we have controlled experimental factors such as voltage, current, pressure, the kind of ambient gases, and the mixture ratio of used gases to optimize the conditions of electric arc discharge for high purity as well as high yield of CNTs.

2. Experimental

MWNTs were prepared by conventional electric arc discharge method. The schematic diagram of dc arc discharge method is shown in Fig. 1. Two graphite rods with a diameter of 10 mm and 25 mm were used as an anode and a cathode, respectively. A voltage of 19-35 V was applied between two electrodes under helium (300-500 torr) or Ar/H_2 mixture (200-350 torr). The MWNTs produced using helium gas were purified by an oxidation in the thermal annealing. The collected samples were first ground into small pieces. The ground samples were then transferred to the annealing furnace. We designed the annealing apparatus, where the inner

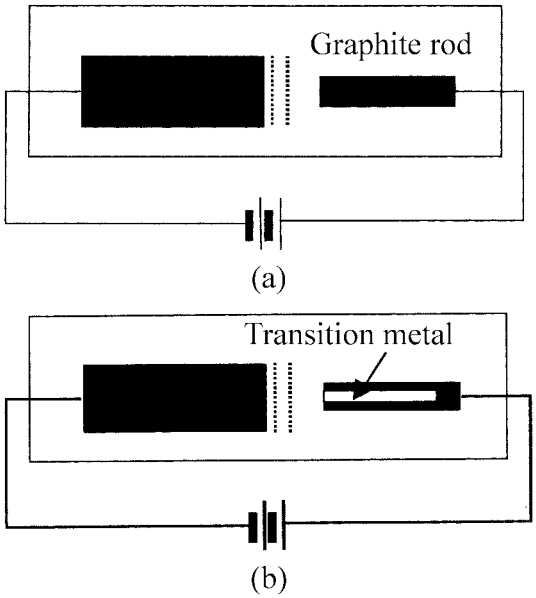

Fig. 1. The schematic diagram of synthesizing MWNT(a) and SWNT(b) by arc discharge.

quartz tube could be rotated. Air was blown into the quartz tube. The inner tube which contained the ground materials was simply rotated by the outer tube that was connected to a step motor with the rate of 30 rpm during the annealing procedure, such that samples were evenly exposed to the surface in order to have uniform selective etching by different oxidation rates controlled exclusively by the annealing time [29]. The inner tube was initially set to a desired temperature prior to the sample loading. We first tried to determine the annealing temperature for fixed annealing time. For temperatures above 760 °C, all samples were burned out quickly. For temperatures below 700 °C, relatively long annealing time was required. In this work, we fixed the annealing temperature at 760 °C and tried to change the annealing time to obtain highly purified samples with high yield. Each time, the raw sample of 100 mg was loaded into the chamber. The yield after the annealing was determined by the weight percentage.

The method for the synthesis of SWNTs are similar to that for the MWNTs, as shown in Fig. 1(b). In this case, the transition metals such as Ni, Fe, and Co and/or their mixtures were used as catalysts. A concentric hole with a diameter of 4 mm was made on the anode and was filled with a mixture of transition metals and a graphite powder. The other graphite rod used as a cathode had a diameter of 25 mm and had a flat surface to keep arc discharge uniformly during the synthesis. This rod was attached to a step-motor, which controlled the distance between two graphite rods by moving forward or backward. The weight percent of total catalysts was fixed to 5%, which is well known to be the optimum ratio of catalysts [12] in graphite rods. The pressure of helium gas was in the range of 100-500 torr.

The morphology of CNTs and the degree of purification were observed by scanning electron microscope (SEM) (JEOL, JSM-6400) and transmission electron microscope (TEM, Hitachi, H-9000NA). Fourier Transform (FT) Raman spectroscopy (BRUKER, RFS 100/S) using Nd : YAG laser (1064 nm) was used to confirm the formation of CNTs and to investigate qualitatively the degree of purification.

Fig. 2. TEM micrograph of MWNTs synthesized under helium pressure of 360 torr.

3. Results and Discussion

Soots deposited on the water-cooled chamber wall mostly contained fullerenes and the carbonaceous particles during the MWNT synthesis. The deposits on the cathode were composed of two parts as a hard outer shell and an soft inner core. The outer shell was hard and gray-colored graphite, where no CNTs were contained. On the other hand, the black inner core contained a plenty of CNTs together with other species such as polyhedral carbon particles and amorphous carbon, etc.

Figure 2 shows the high resolution TEM micrograph of CNTs synthesized under helium pressure of 360 torr. A typical multiwalled CNT is clearly observed in the high resolution TEM micrograph. The synthesized CNTs show the concentric tubes and the evenly spaced layers with equal number of lattice fringes on either side of the central core. The outer diamer of CNTs ranges from about 16 nm to 14 nm, and inner diameter from about 5 nm to 4 nm. The spacing of individual layers is approximately 0.34 nm.

Table 1 shows the length of the burnt-out graphite rod, the deposit length on the cathode, the growth velocity, and the yield as a function of the growth conditions under helium gas. The yields at low bias voltages are larger than that at high bias voltages, although the grown lengths of the deposit at high bias voltages are longer than that at low bias voltages. On the other hand, a little change of the deposit length is observed with increasing pressure. It is found that the optimum growth conditions of MWNTs are the voltage of 20 V and the pressure of 360 torr, where the yield was 93.7%.

Table 1. The length of the burnt-out graphite, the deposit length on the cathode, the growth velocity, and the yield as a function of the growth conditions under helium gas

Voltage [V]	Current [A]	Pressure [torr]	*length of burnt graphite [cm]	deposit length [cm]	growth time [s]	the growth speed of deposit [cm/s]	*yield [%]
35	80	260	5.7	1.6	540	2.96×10^{-3}	28.1
30	80	260	6.5	2.5	480	5.2×10^{-3}	38.5
30	80	360	6.2	2.2	550	4.0×10^{-3}	33
30	80	460	6.2	2.2	600	3.7×10^{-3}	33
20	555	260	1.4	1.2	600	2.0×10^{-3}	85.7
20	555	360	1.6	1.5	600	2.5×10^{-3}	93.7
20	555	460	1.4	1.2	600	2.0×10^{-3}	85.7

*growth velocity = deposit length / time, yield = (deposit length/the length of burnt graphite) $\times$ 100%

Figure 3 shows the SEM images of MWNTs purified by the thermal oxidation as a function of annealing time. Fig. 3(a) is the SEM image of the ground raw sample. MWNTs are rarely seen on the surface after the grinding, since they are mostly embedded inside the carbonaceous particles. The samples are oxidized as a function of time at 760 under air ambient. With annealing for 20 min, some of the carbonaceous particles are removed at the surface and the weight are reduced to about 70 wt% [Fig. 3(b)]. More carbonaceous particles are disappeared by annealing for 30 min [Fig. 3(c)], where the sample weight are reduced to 50 wt%. With annealing for 40 min, major portion of the carbonaceous particles is removed, as shown in Fig. 3(d) and the weight is reduced to about 35 wt%. The purity increases with the increase of annealing time but the yield is expected to be low. During the annealing process, the supply of sufficient amount of oxygen was prerequisite for high purity of nanotubes. However, the temperature of the outer tube was slightly higher at the center than at the edge due to the temperature gradient, prohibiting air flow into the inner tube where the sample was located, although both edges of the outer tube were open to air. The temperature was also important controlling factor, and determined the burn-off rate.

Figure 4 shows the SEM images of the MWNTs produced under different partial pressures of hydrogen gas and argon gas. Fig. 4(a) shows the MWNTs synthesized under total pressure of 200 torr, where the ratio of hydrogen gas to argon gas is 0.33. Many big particles are observed, while

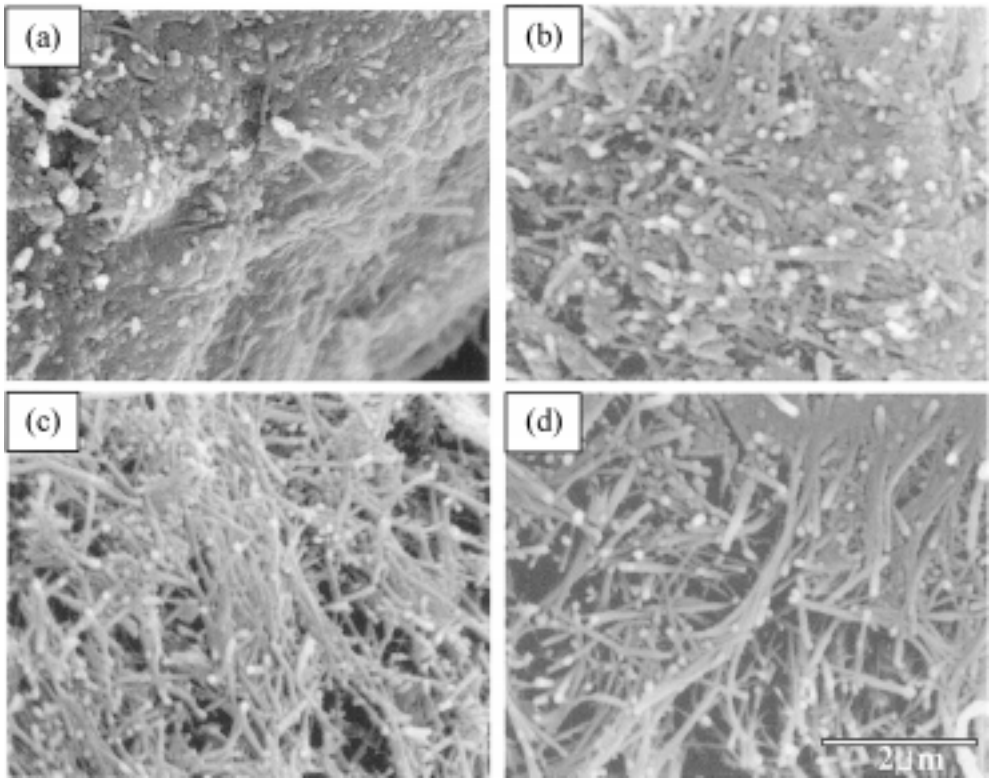

Fig. 3. The SEM images of MWNTs purified by the thermal oxidation at 760°C as a function of annealing time; (a) as-grown, (b) 20 min, (c) 30 min, (d) 40 min.

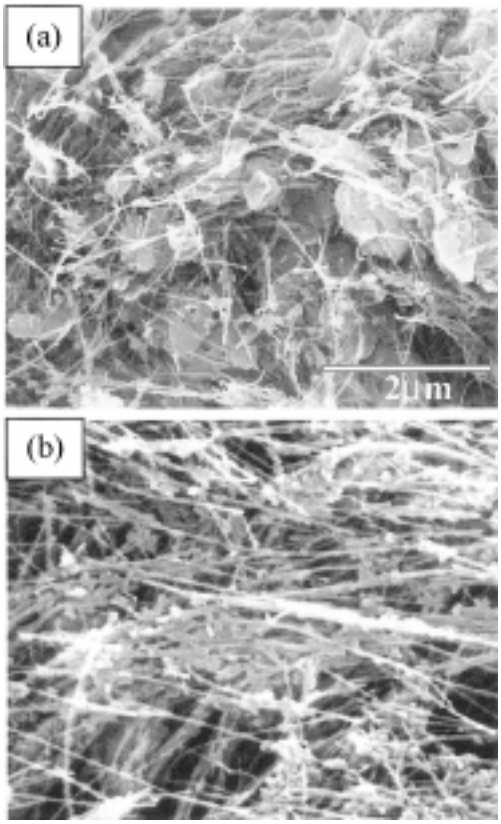

Fig. 4. The SEM images of the MWNTs synthesized under different partial pressures of hydrogen gas and argon gas; (a) 200 torr (H_2: 50 torr, Ar: 150 torr), (b) 275 torr (H_2: 55 torr, Ar: 220 torr).

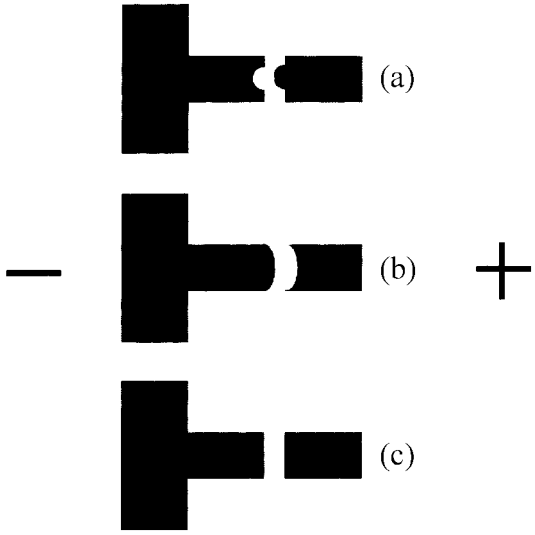

Fig. 5. The schematic shapes of deposits and anodes after the growth as a function of the ratio of hydrogen gas to argon gas; (a) less than 1/4, (b) more than 1/4, (c) equal to 1/4.

MWNTs are not abundant. The length of the MWNTs is micrometer scale and the diameter is smaller than those of MWNTs synthesized under helium gas due to hydrogen etching of the walls of MWNTs. Fig. 4(b) shows the MWNTs produced under a total pressure of 275 torr, where the ratio of hydrogen gas to argon gas is 0.25. The MWNTs synthesized under 275 torr are more straight than those under 200 torr, and the big carbonaceous particles are rarely to be seen. The mean free path of hydrogen gas under low total pressure (200 torr)

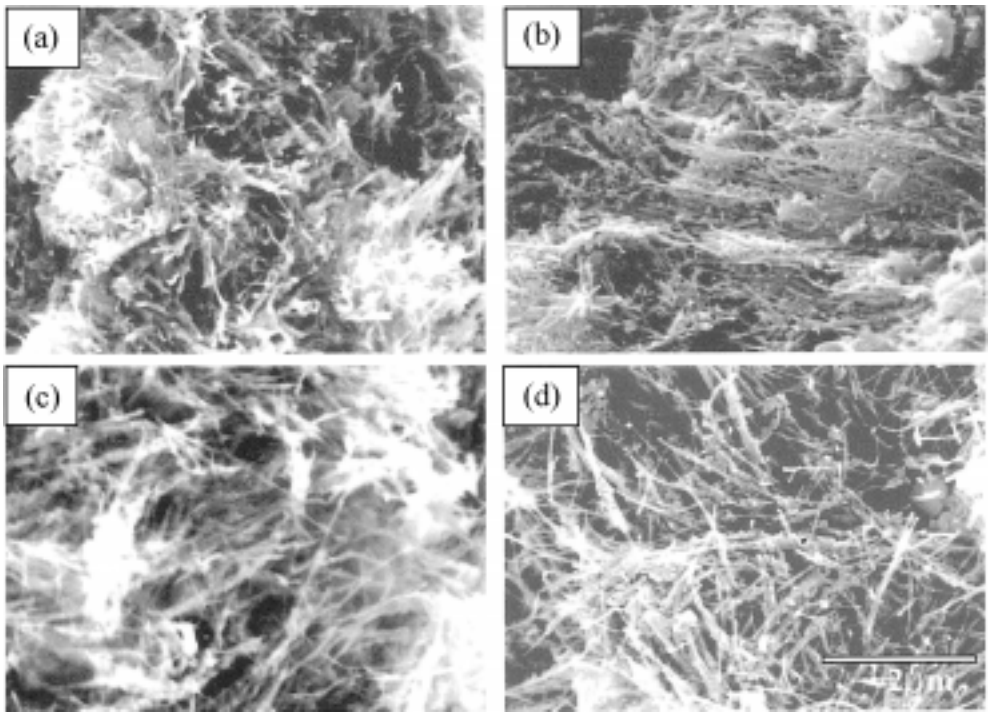

Fig. 6. The SEM images of MWNTs synthesized under various total pressure, where the ratio of hydrogen gas to argon gas is fixed to 0.25; (a) 200 torr, (b) 250 torr, (c) 300 torr, and (d) 350 torr.

with the higher ratio of hydrogen gas (0.33) are much longer than that under high total pressure (275 torr) with the low ratio of hydrogen gas (0.25). These neutral atoms or ions have very high energies, and they make the big graphite layers peeled off rapidly from the graphite rods. Therefore, lots of big carbonaceous particles are easily produced as shown in Fig. 4(a).

Figure 5 shows the schematic shapes of deposits and anodes after the growth as a function of the ratio of hydrogen gas to argon gas. When the mixing ratio is less than 0.25, the inner part of the anode is left unburned, as shown in Fig. 5(a). On the other hand, the deposits on the cathode at the central part are dug, as shown in the figure. The gray-colored hard part is produced at the center of the deposit, and no nanotubes are observed. When the ratio is higher than 0.25, the deposits on the cathode has a concave shape, as shown in Fig. 5(b). However, the gray-colored hard part is not observed at the center of the deposit. With the ratio of 0.25, both the deposit and the anode are flat, and the gray-colored hard part an the center of the deposit is not produced. It is noted that the optimum ratio of hydrogen to argon for the synthesis of MWNTs is 0.25.

Figure 6 shows the SEM images of MWNTs synthesized under various total pressure (200-350 torr), where the ratio of hydrogen gas to argon gas is fixed to 0.25. The synthesized MWNTs show almost the same morphology and yield, regardless of the total pressure. However, with increasing the pressure, the purity of MWNTs increases gradually. This suggests that hydrogen plasma etches away the carbonaceous particles.

Figure 7 represents the Raman spectra of the MWNT samples shown in Fig. 6. The peaks around 1280 cm^{-1} called as the D-mode, are known to be attributed to amorphous carbons and defects of nanotubes, whereas the peaks around 1600 cm^{-1} called as the G-mode are known to be due to the graphitic structure of carbon atoms. The G-mode of produced MWNT is shifted to lower wave number region (1582 cm^{-1}) by the strain of forming tube. The intensity of the peak at 1285 cm^{-1} decreases with increasing the pressure of

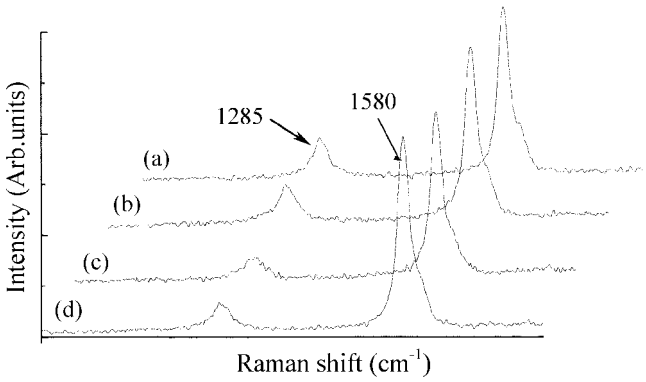

Fig. 7. Raman specra of MWNTs synthesized under various total pressure, where the ratio of hydrogen gas and argon gas is fixed to 0.25; (a) 200 torr, (b) 250 torr, (c) 300 torr, and (d) 350 torr.

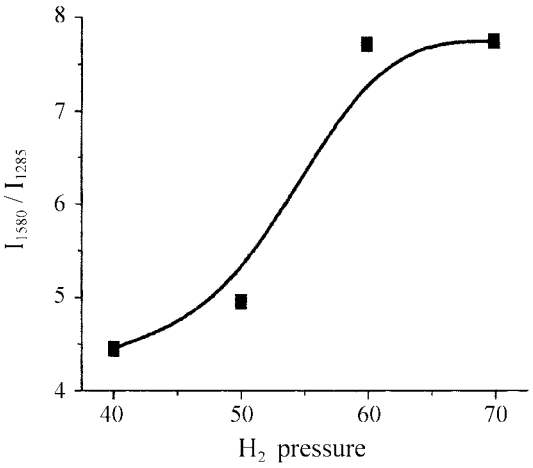

Fig. 8. The ratio of G-mode to D-mode in Raman specra of MWNTs synthesized as a function of partial pressures of hydrogen.

hydrogen gas. It is clearly noted that the ratio of the G-mode to the D-mode increases with increasing the pressure of hydrogen gas, as shown in Fig. 8. The MWNT synthesized under total pressure of 350 torr (70 torr of hydrogen gas) shows the best purity among grown MWNTs.

In the synthesis of SWNTs, the gray-colored bar produced

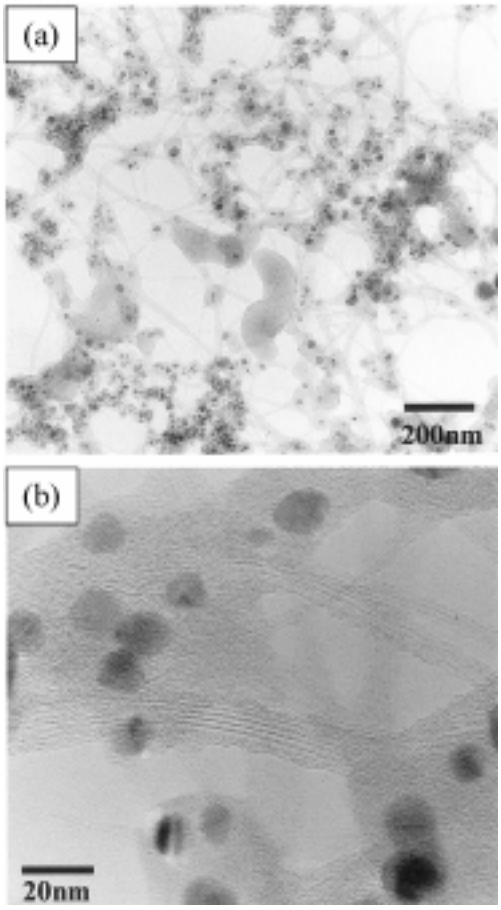

Fig. 9. TEM images of the SWNTs grown in collar part under 100 torr; (a) moderate magnification, (b) higher magnification

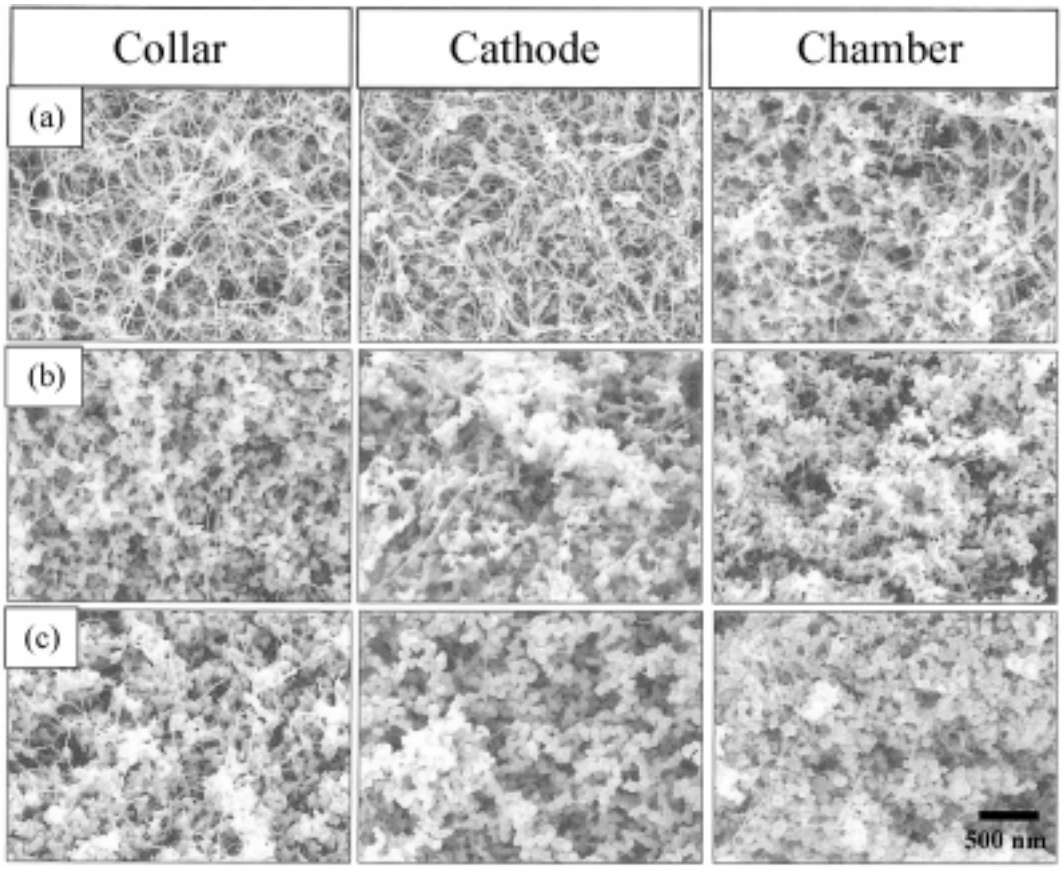

Fig. 10. The SEM images of the SWNTs collected on the collar, the cathode, and chamber, synthesized under different helium pressure; (a) 100 torr, (b) 300 torr, (c) 500 torr.

at the center of the cathode, called as the deposit, contained no SWNTs. The messy part except the deposit on the flat plane of the cathode was called as a collar. It has been known that the purity of SWNTs at the collar is the highest. The round part on the cathode was called as cathode and web-like soots could be seen in it. The black sheet-like soots called as rubbery soots were attached to the chamber. The SWNTs on the chamber were the major portion among the total yield of the produced SWNTs. Therefore, in order to produce the large scale and low cost synthesis of SWNTs by the arc discharge, it is necessary to increase the yield and purity of these rubbery soots.

Figure 9 shows the TEM image of the SWNTs grown on the collar part under 100 torr. It can be seen that the appearance of SWNTs is quite different from that of MWNTs as shown in Fig. 2. The individual tubes have very small diameters (about 1.4 nm) and are curled and looped rather than straight. SWNTs are usually formed in bundles, which are composed of one to tens of SWNTs. The bundles are contaminated with amorphous carbon and catalytic particles whose diameters are 5~10 nm.

Figure 10 shows the SEM images of SWNTs collected on the collar, the cathode, and chamber, synthesized with 5 wt% of catalyst mixtures of nickel, iron, and cobalt under a helium pressure of 100~300 torr. Regardless of helium pressure, the purity of SWNTs increases in the order of collar, cathode and chamber. Most of carbonaceous particles in the collar part are attached to the ends of the bundles of SWNTs, as shown in Fig. 10(a). The round-type carbonaceous particles are attached to the junction of bundles in the collar part, whereas these are expanded to the side of bundles in the cathode and chamber. The diameter of the bundles is in the range of 10-20 nm. It is noted that the purity of SWNTs increases with decreasing the helium pressure. The collar part synthesized at a helium pressure of 100 torr shows the best purity among all other samples. It is proposed that graphite powders with transition metal particles are easily vaporized at low pressure, resulting in the promotion of the chance for diffusion of carbon atoms into the catalytic particles. Therefore, the nanotubes are easily synthesized at low pressure of helium.

4. Conclusions

We have investigated the synthetic methods for high purity and high yield of MWNT and SWNT by arc discharge. MWNTs were synthesized under different pressures of helium and the gas mixture of argon and hydrogen. Relatively high pressure of 300-400 torr is required for high yield MWNTs synthesis at low bias voltage of about 20 V and 55 A, whereas low pressure of about 100 torr is required for

SWNTs. Introduction of the hydrogen gases during the synthesis of the MWNTs improves the yield and purity of the samples. The SWNTs are synthesized by the assistance of a small amount of mixture of transition metals, which played as a catalyst during the formation process. The purity and yield of the SWNTs are higher at lower pressure and enhanced by mixing more components of the transition metals.

References

[1] Iijima, S. *Nature* **1991**, *354*, 56.
[2] Dillon, A. C.; Jones, K. M.; Bekkedahl, T. A.; Kiang, C. H.; Bethune, D. S.; Heben, M. J. *Nature* **1997**, *386*, 377.
[3] Wu, X. B.; Chen, P.; Lin, J.; Tan, K. L. *Hydrogen Energy.* **2000**, *25*, 261.
[4] Niu, C.; Sichel, E. K.; Hoch, R.; Moy, D.; Tennent, H. *Appl. Phys. Lett.* **1997**, *70*, 1480.
[5] Ma, R. Z.; Liang, J.; Wei, B. Q.; Zhang, B.; Xu, C. L.; Wu, D. H. *J. Power Source*. **1999**, *84*, 126.
[6] Wu, G. T.; Wang, C. S.; Zhang, X. B.; Yang, H. S.; Qi, Z. F.; Li, W. Z. *J. Power Source*. **1998**, *75*, 175.
[7] Dai, H.; Hafner, J. H.; Rinzler, A. G.; Colbert, D. T.; Smalley, R. E. *Nature* **1996**, *384*, 147.
[8] Wong, S. S.; Wolley, A. T.; Joselevich, E.; Cheung, C. L.; Lieber, C. M. *J. Am. Chem. Soc.* **1998**, *120*, 8557.
[9] Dai, H.; Franklin, N.; Han, *J. Appl. Phys. Lett.* **1998**, *73*, 1508.
[10] Roschier, L.; Penttila, J.; Martin, M.; Hakonen, P.; Paalanen, M. *Appl. Phys. Lett.* **1999**, *75*, 728.
[11] Yao, Z.; Postma, H. W. C.; Balents, L.; Dekker, C. *Nature* **1999**, *402*, 273.
[12] Hu, J. T.; Min, O. Y.; Yang, P. D.; Lieber, C. M. *Nature* **1999**, *399*, 48.
[13] Fan, S.; Chapline, M. G.; Franklin, N. R.; Tombler, T. W.; Cassell, A. M.; Dai, H. *Science* **1999**, *283*, 512.
[14] Wang, Q. H.; Seltlur, A. A.; Lauerhaas, J. M.; Dai, J. Y.; Seelig, E. W.; Chang R. P. H. *Appl. Phys. Lett.* **1998**, *72*, 2912.
[15] Xu, X.; Brandes, G. R. *Appl. Phys. Lett.* **1999**, *74*, 2549.
[16] Ebbesen, T. W. *Nature* **1992**, *358*, 220.
[17] Tomita, M.; Saito, Y.; Hayashi, T. *Jap. J. Appl. Phys.* **1993**, *32*, L280.
[18] Bethune, D. S.; Kiang, C. H.; Vries, M. S.; Gorman, G.; Savoy, R.; Vasquez, J. *Nature* **1993**, *363*, 605.
[19] Iijima, S.; Ichihashi, T. *Nature* **1993**, *363*, 603.
[20] Dai, H.; Rinzler, A. G.; Nikolaev, P.; Thess, A.; Colbert, D. T.; Smalley, R. E. *Chem. Phys. Lett.* **1996**, *260*, 471.
[21] Guo, T.; Nikolaev, P, Thess, A.; Colbert, D. T.; Smalley, R. E. *Chem. Phys. Lett.* **1995**, *249*, 49.
[22] Hsu, W. K.; Hare, J. P.; Terrones, M.; Kroto, H. W.; Walton, D. R. M ; Harris, P. J. F. *Nature* **1995**, *377*, 687.
[23] Hsu, W. K.; Hare, J. P.; Terrones, M.; Kroto, H. W.; Walton, D. R. M. *Chem. Phys. Lett.* **1996**, *262*, 161.
[24] Cheng, H. M.; Li, F.; Su, G.; Pan, H. Y.; He, L. L.; Sun, X.; Dresselhaus, M. S. *Appl. Phys. Lett.* **1998**, *72*, 3282.
[25] Bonard, J. M.; Stora, T.; Salvetat, J. P.; Maier, F. *Advanced Materials* **1997**, *9*, 827.
[26] Duesburg, G. S.; Burghard, M.; Muster, J.; Philipp G.; Roth, S. J. *Chem. Soc., Chem. Commun.* **1998**, 435.
[27] Ikazaki, F.; Ohshima, S.; Uchida, K.; Kuriki, Y.; Hayakawa, H.; Yumura, M. *Carbon* **1994**, *32*, 1539.
[28] Tohji, K.; Goto, T.; Takahashi, H.; Shinoda, Y.; Shimizu, N.; Jeyadevan, B. *Nature* **1996**, *383*, 679.
[29] Park, Y. S.; Choi, Y. C.; Lee, Y. H.; An, K. H. et al. *Carbon* **2000**, *in press*.